HITTITE JOURNAL OF SCIENCE AND ENGINEERING

e-ISSN: 2148-4171
Volume: 11 • Number: 4
December 2024

High-Precision UAV Photogrammetry with RTK GNSS: Eliminating Ground Control Points

Mehmet Nurullah Alkan
Hitit University, Osmancık Ömer Derindere Vocational High School, 19500, Çorum, Türkiye.

Corresponding Author
Mehmet Nurullah Alkan
E-mail: nurullahalkan@hitit.edu.tr Phone: +90 530 511 56 69 Fax: +90 364 611 50 30
RORID: https://ror.org/01x8m3269

Article Information
Article Type: Research Article
Doi: https://doi.org/10.17350/HJSE19030000341
Received: 12.08.2024
Accepted: 24.09.2024
Published: 31.12.2024

Cite As
Alkan M, N. High-Precision UAV Photogrammetry with RTK GNSS: Eliminating Ground Control Points. Hittite J Sci Eng. 2024;11(4):139-147.

Peer Review: Evaluated by independent reviewers working in at least two different institutions appointed by the field editor.
Ethical Statement: Not available.
Plagiarism Checks: Yes - iThenticate
Conflict of Interest: Author approves that to the best of his knowledge, there is not any conflict of interest or common interest with an institution/organization or a person that may affect the review process of the paper.

CRediT AUTHOR STATEMENT
Mehmet Nurullah Alkan: Conceptualization, Methodology, Software, Validation, Writing- original draft, Data curation, writing-review and editing, Investigation.

High-Precision UAV Photogrammetry with RTK GNSS: Eliminating Ground Control Points

Mehmet Nurullah Alkan

Hitit University, Osmancık Ömer Derindere Vocational High School, 19500, Çorum, Türkiye.

Abstract

The advancements in Unmanned Aerial Vehicles (UAVs) have significantly enhanced the capability of the photogrammetric approaches, particularly with the integration of Real-Time Kinematic (RTK) sensors. That approach enables the operators to use the Global Navigation Satellite System (GNSS) more efficiently with the production of high-precision 3D Digital Terrain Models (DTMs). Traditionally, Ground Control Points (GCPs) are used to link those models to a ground coordinate system, but their establishment is time-consuming and labor-intensive, requiring static or rapid-static GNSS observations over two hours for each point. However, RTK-embedded UAVs offer a significant improvement by facilitating direct geo-referencing of DTMs, which includes the estimation of internal and external orientation parameters more efficiently and potentially eliminating the need for GCPs.

In this study, UAV flights over a test area at various altitudes (30m, 45m, 60m) were conducted to evaluate the 3D positioning accuracy of photogrammetric models generated without using any GCP, and their locations were compared against the precise GNSS observations for 22 control points. Results indicated that UAVs with RTK ability could achieve centimeter-level accuracy in positioning, making this kind of evaluation a viable alternative to traditional methods. This study also discusses the implications of those results within the context of large-scale map production and their regulations in Türkiye. The elimination of GCPs should significantly reduce the time and effort associated with map production, suggesting a potential alternative in regulatory standards to incorporate these technological approaches.

Keywords: UAV, RTK GNSS, photogrammetry, direct geo-referencing, 3D modeling, GCP, Türkiye mapping regulations.

INTRODUCTION

In order to implement field observations, there are several methods using different technologies or approaches. The main issue for those positional evaluations arises from the required precision of the subject, the offered accuracy of the method and the accomplished detail level of the scene (building, field, etc.), whether it is a direct technique or an indirect method. In this context, total station, Global Navigation Satellite System (GNSS), laser-scanning and terrestrial/aerial photogrammetry are the most common procedures today. However, the final solution for all those methods includes the representation of the field, whether by a 2D/3D point cloud (laser scanning and photogrammetry) or the characteristic edges of the scene material (total station and GNSS) (1-4).

Unmanned Aerial Vehicles, known as UAVs or drones, are commonly used in many applications to acquire point clouds, which include high-precision observations of an area. With the possibility of collecting digital images and technological advancements within UAVs, it is possible to create a 3D model of a ground surface in a short time period economically using an aerial photogrammetric approach (5-7). This technique requires less expensive equipment and minimal time-consuming process in the field compared to the other mentioned methods above with several advantages, which include:

- High-precision and dense point cloud data,
- Economic evaluation of metric information from the 3D model (volume, area, etc.),
- Repeated measurements on the model at any time without new flights or processes (6-9).

During the process, acquired data including overlapped images from the field lead to the creation of point clouds, orthophoto maps and DTMs which can be used in mapping, inspection of constructions, emergency applications, archaeology, architecture, monitoring topographic alterations, preservation of cultural heritage, etc. (4, 10-15). The main output of those photogrammetric procedures includes the processing of multi-spectral, thermal, or visible-light images taken at regular intervals from the scene and linking them to the ground coordinate system. That process is defined as “georeferencing” and has two different approaches: (i) direct and (ii) indirect georeferencing. The direct method is implemented by using the camera’s position information collected by an onboard GNSS receiver. The other method can be performed by using the coordinates of specific points (GCPs) on the ground but requires additional observations on the field. The accuracy of those methods generally depends on the flight route and height, image resolution, and especially preferred georeferencing solution. Either way, those approaches enable operators to link their 3D model to the ground truth, which is produced by Structure from Motion (SfM), a multi-image photogrammetry technique, and have an arbitrary reference coordinate system for the final outputs (6-7, 9, 14, 16-18).

The 3D positioning accuracy of a UAV model strongly depends on the GNSS type used on the board. If the GNSS sensor has the ability to process code-based signals, the accuracy is about ±5-10 m in both horizontal and vertical directions, but the capability to use dual-frequency satellite signals enables the procurement of cm-level 3D positioning (7, 18-20). The first case requires additional fieldwork. Here, GCPs are essential to convert the photogrammetric model into a ground coordinate system by scaling the whole cloud of points, and according to the current regulations in Türkiye, one should conduct at least 2 hours of GNSS observations (rapid-static surveys) on all of the GCPs in the scene (6, 21). There is no consensus on the number and distribution of the GCPs in a scene, but some theoretical studies indicate that a well-distributed 5-10 GCPs are sufficient to create a 3D model independent from the area of the process. If the number of GCPs increases, operating costs will also rise accordingly (4, 7, 22). The other case can be achieved by using UAVs with Real-Time Kinematic (RTK) capabilities which allow the collection

of field data with direct georeferencing. That situation eliminates the need for GCPs (4, 23-25).

Photogrammetric solutions based on either of those approaches have specific drawbacks inherent to the techniques themselves. They include gathering permissions for each flight, weather conditions, flight duration, time window during the daylight, GCP establishment and observation via GNSS, etc., and the after-flight process of constructing a DTM. Nevertheless, a general evaluation of those methods indicates that GCP establishment in the field is the most prominent obstacle to 3D model creation (18, 26-29).

In this study, the positional accuracy of three different models generated from UAV flights at altitudes of 30, 45, and 60 meters over a test field were tested against GNSS observations on the same object points. The position data of those points were generated using the photogrammetric point clouds, and the correlation with the reference coordinates was examined. That situation enables the test for whether the photogrammetric models could achieve the theoretical accuracy of GNSS observations based on the Continuously Operating Reference Stations (CORS (TUSAGA-AKTİFTR)) system (23). Additionally, the necessity of GCPs, which are considered C3-level reference points according to regulations in Türkiye and used for georeferencing, was comparatively analyzed. UAV-based photogrammetry in large-scale mapping and terrestrial positioning projects was also evaluated, while the effects of UAV flight altitudes on the current map production accuracy were examined in detail. This study also aims to evaluate the accuracy and reliability of UAV-based photogrammetric methods and to reveal their compatibility with terrestrial GNSS measurements. Additionally, by discussing the role and necessity of GCPs in photogrammetric processes, important insights into how those technologies can be used more effectively within the framework of existing regulations in Türkiye were presented.

METHODOLOGY

Test field assessment and CP selection

To compare GNSS observations with the UAV photogrammetric model in terms of precision, an area with prominent markers was selected (Figure 1). This test field is the parking lot of the Faculty of Science and Literature at Hitit University in Çorum Province, Türkiye, and was chosen due to the presence of distinctive and well-distributed markers.

The absence of obstacles at the specified flight altitudes is another reason for selecting this site. Also, the calculated ground height of selected Control Points (CP) were used with their original computed elevation, because no embossed paint was applied. One can assume that this situation in the field simulates real-world conditions often encountered in practice for distinctive objects, such as road edges, field boundaries, and building corners. Therefore, CPs are selected as features like road edge lines and arrows (Figure 2).

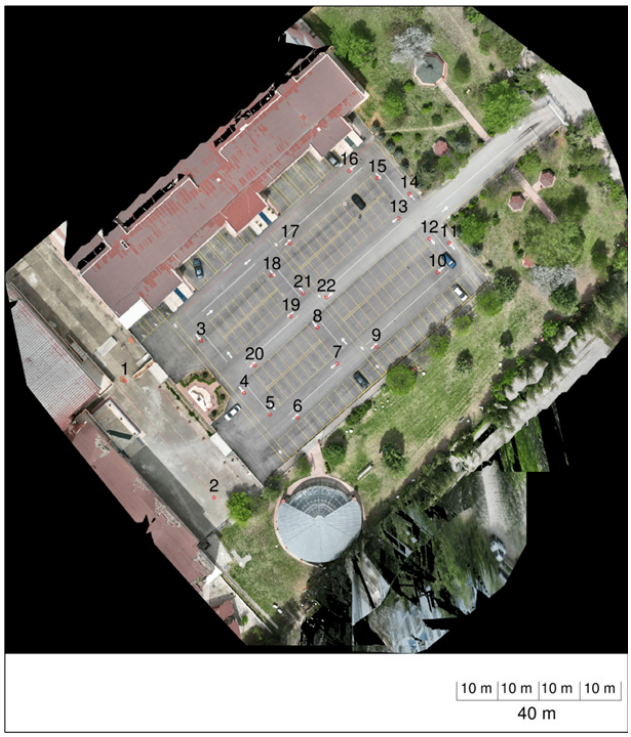

Figure 1 Test field used in this study. A well-distributed set of 22 points was chosen from the parking lot (mostly covered with straight lines and arrows).

Figure 2 West side of the parking lot from 30 m flight altitude. CPs on this part of the field were marked with red circles (CPs 3-6 and 20).

GNSS observations

A total of 22 distinctive objects in the field were selected as CPs, and their coordinates were calculated as the average of two different GNSS sessions with one-hour intervals. During the process, a GNSS receiver compatible with the CORS-TR network was used, and calculated positions of the CPs were considered as reference coordinates for further evaluation. Such observations are considered as RTK or Network-RTK, according to the used base stations. This is accomplished by using a base station (via RTK) or a whole network (Network-RTK) that sends correction vectors to the rover (in this case GNSS receiver and UAV) and applying those values to precisely generate the 3D position. Network-RTK observations, preferred to collect the reference coordinates in this study, offer real-time corrections for centimeter-level accuracy theoretically. Although current regulations in Türkiye suggest a minimum of 3 epochs for detail points, 10 epochs of

observations were executed for each session, adhering to the primary criterion for polygon coordinate calculations (21, 31).

UAV flights

Autonomous flights over the field were performed with a UAV with RTK capability at altitudes of 30, 45, and 60 meters. The UAV used in this study was the DJI Mavic 3 Enterprise, which offers robust performance with a weight of 915 grams and a maximum flight speed of 15 m/s. It is equipped with a GNSS system which can operate with multiple satellite constellations, and a wide camera sensor with a resolution of 20 megapixels, producing images up to 5280 x 3956 pixels. The UAV's gimbal stabilization is three-axis, ensuring stable and clear images and the RTK module positioning accuracy is within 1 cm + 1 ppm horizontally and 1.5 cm + 1 ppm vertically (Table 1).

Table 1 Key specifications of the UAV used in this study (URL-5).

Brand/Model	DJI/Mavic 3 Enterprise
Weight	915 g
Max flight speed	15 m/s
Used GNSS	GPS+Galileo+BeiDou+GLONASS
Wide camera sensor	4/3 CMOS, 20 MP
Max image size	5280x3956
Gimbal stabilization	3-axis
RTK module positioning accuracy (RTK Fix)	Horizontal: 1 cm + 1 ppm Vertical: 1.5 cm + 1 ppm

During the UAV flights, a GNSS receiver inside the parking lot is used as a reference station. In this step, a random location for the point was selected, and 3D coordinates were computed with a 60-epoch observation. The coordinates were then used as reference coordinates for all the photogrammetric models. Then, the GNSS receiver was linked to the UAV control unit and started to send correction values via Bluetooth during the flights.

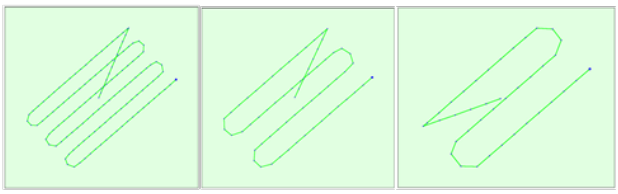

Figure 3 Top view of the flight routes and initial image positions for 30-45-60m flights, respectively. The green line represents the flight route of the UAV, with a big blue dot (starting point) and black dots (camera positions). Direct lines from the last points of the routes to the center of the models represent the UAV height correction route. That feature enables the collection of images with a 45-degree camera angle and develops the estimation of the whole model's elevation data (URL-5).

A total of 138, 65, and 39 digital images were collected during the autonomous flights at 30 m, 45 m, and 60 m altitudes, respectively. Forward and side image overlap ratios were selected as 80% and 70% respectively, to ensure an accurate 3D photogrammetric model of the field with a 90-degree camera angle. The camera, which is embedded in the UAV (M3E_12.3 RGB), provides sufficient resolution for all flights in the study; and the ground sampling distance (GSD), area covered, and the number of images for each flight altitude detailed in Table 2. This setup ensured comprehensive coverage and high-resolution data collection for subsequent photogrammetric processing (Figure 3, 4, 5).

Table 2 Specifications of flight altitudes. Processed areas differ from each other; thus, the flight altitudes enable to collect images with a larger perspective as the height increases. This situation has a drawback on the Ground Sampling Distance.

Flight Altitude	Ground Sampling Distance (GSD)	Area Covered	Number of Images
30 m	0.85 cm	1.6673 ha.	138
45 m	1.27 cm	2.3190 ha.	65
60 m	1.68 cm	3.2324 ha.	39

Photogrammetric model generation

To generate a 3D DTM of a field, third-party applications such as Agisoft Photoscan, Pix4D, and Terra can be used. Those software programs can process all the aerial digital images with aerial triangulation and bundle block adjustment procedures to generate ortho-mosaic maps and point clouds. In this study, Pix4D was selected for all the digital processing steps. That software enables users to create point clouds, orthophotos, and accurate DTMs from aerial images (7, 9, 22, 33). The generated point clouds then were used to derive the 3D coordinates of the CPs.

The processed data enables high-resolution ortho-mosaic images and detailed DTMs for each flight altitude, and those are critical for assessing the accuracy and reliability of the photogrammetric models. The ortho-mosaic images provide a precise and geometrically corrected view of the field, ensuring that spatial relationships are accurately represented. The DTMs, on the other hand, represent the elevation data of the field's surface, capturing the subtle variations in height that are crucial for various analytical purposes (Figure 4).

In Figure 4, details and covered area have an inverse proportion; as the altitude increases, the area increases, but resolution decreases as expected. That can be observed clearly on the roof of the building in the north-west.

In order to assess the reliability of the models, geolocation variance for all flights has significant importance (Table 3). Those values indicate the difference between the

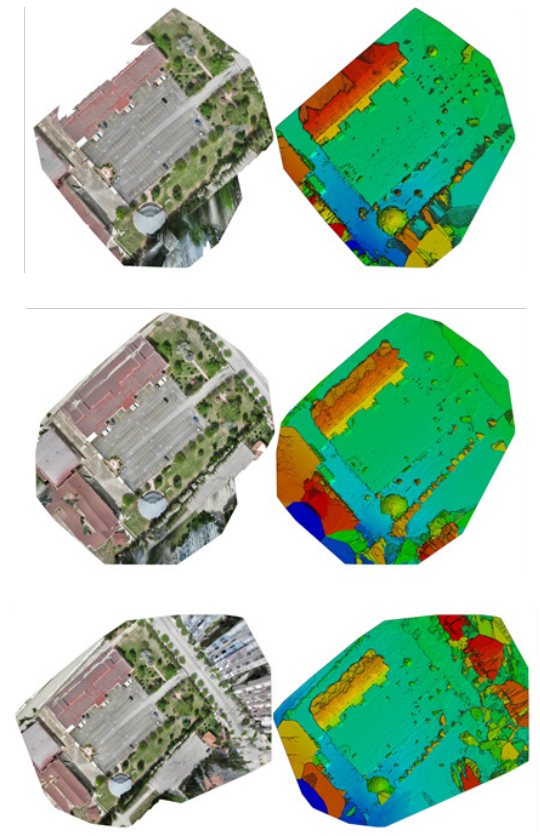

Figure 4 Ortho-mosaic and DTM were generated for 30-45-60m UAV flights, respectively.

According to Table 3, even with the higher altitudes up to 60 m, the 3D positional accuracy of the models is adequate for further evaluation. Also, all the geolocation errors are below 1 cm, but vertical accuracy might need careful consideration. Overall, the 45m flight offers the best correlation between horizontal and vertical precision.

Table 3 Geolocation errors for all photogrammetric models.

	Geolocation Error X	Geolocation Error Y	Geolocation Error H
RMS Error (m) [30 m]	0.005488	0.006392	0.006464
RMS Error (m) [45 m]	0.004127	0.004216	0.005418
RMS Error (m) [60 m]	0.003225	0.003213	0.007683

Data comparison and discussion

To analyze the differences between the ground truth at the 22 CPs and the photogrammetric models, all data was evaluated to determine if they have a normal distribution or not. For this purpose, the Shapiro-Wilk test was executed to assess the normality of the differences in all 3 axes, and the Paired t-test and Wilcoxon tests were applied, when necessary, to figure out if there was a systematic diversity (34-36). In addition, the mean error, root mean square error (RMSE), and standard deviations (σ) were calculated for each coordinate diversity pair to verify the variability and reliability of the photogrammetric models. Those analyses are crucial for evaluating the accuracy and reliability. Specifically, the mean error indicates the degree of deviation in the models, while the RMSE and σ values are important metrics for assessing the overall accuracy and data dispersion.

RESULTS

The average coordinates of two different GNSS sessions for 22 different CPs in the field were accepted as the reference coordinates. Subsequently, the coordinates of those points were calculated from each point cloud generated using Pix4D software for the 30, 45 and 60 m flights (22). As expected, there are distinctive differences in the Y, X, and H coordinates between the data sets (Table 4, Figure 5).

According to Table 4, the differences are below the specified values required by regulations in Türkiye (21). Maximum deviation and mean error for all axes promote the situation. Specifically, elevations for all altitudes indicate a careful approach for this axis.

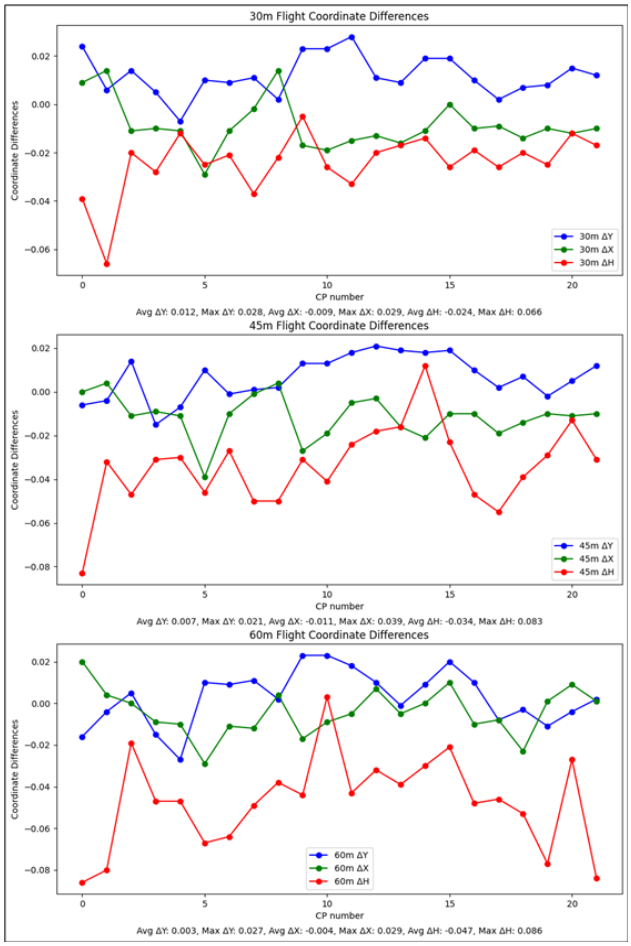

Figure 5. Coordinate differences for all axes. Average and maximum deviations (as absolute value) are given under the graphs.

Table 4. CP Coordinate differences between GNSS observations and photogrammetric models.

	30m flight			45m flight			60m flight		
#	**ΔY(m)**	**ΔX(m)**	**ΔH(m)**	**ΔY(m)**	**ΔX(m)**	**ΔH(m)**	**ΔY(m)**	**ΔX(m)**	**ΔH(m)**
1	0.024	0.009	-0.039	-0.006	0.000	-0.083	-0.016	0.020	-0.086
2	0.006	0.014	-0.066	-0.004	0.004	-0.032	-0.004	0.004	-0.080
3	0.014	-0.011	-0.020	0.014	-0.011	-0.047	0.005	0.000	-0.019
4	0.005	-0.010	-0.028	-0.015	-0.009	-0.031	-0.015	-0.009	-0.047
5	-0.007	-0.011	-0.012	-0.007	-0.011	-0.030	-0.027	-0.010	-0.047
6	0.010	-0.029	-0.025	0.010	-0.039	-0.046	0.010	-0.029	-0.067
7	0.009	-0.011	-0.021	-0.001	-0.010	-0.027	0.009	-0.011	-0.064
8	0.011	-0.002	-0.037	0.001	-0.001	-0.050	0.011	-0.012	-0.049
9	0.002	0.014	-0.022	0.002	0.004	-0.050	0.002	0.004	-0.038
10	0.023	-0.017	-0.005	0.013	-0.027	-0.031	0.023	-0.017	-0.044
11	0.023	-0.019	-0.026	0.013	-0.019	-0.041	0.023	-0.009	0.003
12	0.028	-0.015	-0.033	0.018	-0.005	-0.024	0.018	-0.005	-0.043
13	0.011	-0.013	-0.020	0.021	-0.003	-0.018	0.01-2	0.007	-0.032
14	0.009	-0.016	-0.017	0.019	-0.016	-0.016	-0.001	-0.005	-0.039
15	0.019	-0.011	-0.014	0.018	-0.021	0.012	0.009	0.000	-0.030
16	0.019	0.000	-0.026	0.019	-0.010	-0.023	0.020	0.010	-0.021
17	0.010	-0.010	-0.019	0.010	-0.010	-0.047	0.010	-0.010	-0.048
18	0.002	-0.009	-0.026	0.002	-0.019	-0.055	-0.008	-0.008	-0.046
19	0.007	-0.014	-0.020	0.007	-0.014	-0.039	-0.003	-0.023	-0.053
20	0.008	-0.010	-0.025	-0.002	-0.010	-0.029	-0.011	0.001	-0.077
21	0.015	-0.012	-0.012	0.005	-0.011	-0.013	-0.004	0.009	-0.027
22	0.012	-0.010	-0.017	0.012	-0.010	-0.031	0.002	0.001	-0.084

Table 5. Tests for coordinate differences. According to Shapiro-Wilk test results, Paired t-test was applied to 30 m (Y) and 45 m (Y, X, H) flights. Values without normal distribution are evaluated through Wilcoxon test.

Metric	30m	45m	60m
Shapiro-Wilk Test (Y)	W=0.9707, p=0.7282	W=0.9543, p=0.3826	W=0.9693, p=0.6955
Shapiro-Wilk Test (X)	W=0.8644, p=0.0062	W=0.9283, p=0.1129	W=0.9825, p=0.9507
Shapiro-Wilk Test (H)	W=0.8475, p=0.0031	W=0.9510, p=0.3303	W=0.9643, p=0.5808
Paired t-test (Y)	t=6.632, p=1.449e-06	t=3.1813, p=0.0045	-
Paired t-test (X)	-	t=-5.3123, p=0.0000	-
Paired t-test (H)	-	t=-8.5361, p=0.0000	-
Wilcoxon Test (Y)	-	-	W=92.5, p=0.2902
Wilcoxon Test (X)	W=33.0, p=0.0041	-	W=59.5, p=0.0893
Wilcoxon Test (H)	W=0.0, p=4.768e-07	-	W=1.0, p=9.536e-07

At this step, it is necessary to statistically evaluate whether those differences are significant or systematic. For this purpose, the Shapiro-Wilk test was initially used to determine whether the coordinate differences for all three axes have a normal distribution or not (35). The components with a normal distribution ($p>0.05$) were assessed using the Paired t-test, while those without a normal distribution ($p\leq0.05$) were evaluated by a non-parametric (Wilcoxon) test (34, 36). For this purpose, the test results for each flight at 30, 45, and 60 meters were examined (Table 5).

The results of the Shapiro-Wilk test indicated that only the Y coordinate differences at 30m and all axes for 45m have a normal distribution. The paired t-test results showed significant differences in the Y axis at 30m and in the Y, X, and H axes at 45m. Also, 60m altitude does not have a normal distribution; thus, the Wilcoxon test is applied for this flight route. The analysis of the differences in coordinates obtained from GNSS and photogrammetric methods for flights from 30 m and 45 m altitudes indicates varied statistical significance. That leads to systematic differences amongst them. Despite those differences, RMSE and σ values indicate that both the photogrammetric model and GNSS measurements are generally consistent and reliable, and systematic errors may arise from the uncertainty in the RTK technique (Figure 6). However, the photogrammetric model from the 60 m flight altitude exhibits different characteristics from the other models. In this case, coordinate differences along Y and X axes are not significant, indicating random errors around this

flight route and no systematic error. Also, height coordinate observations require careful examination due to their higher variability across all the photogrammetric models.

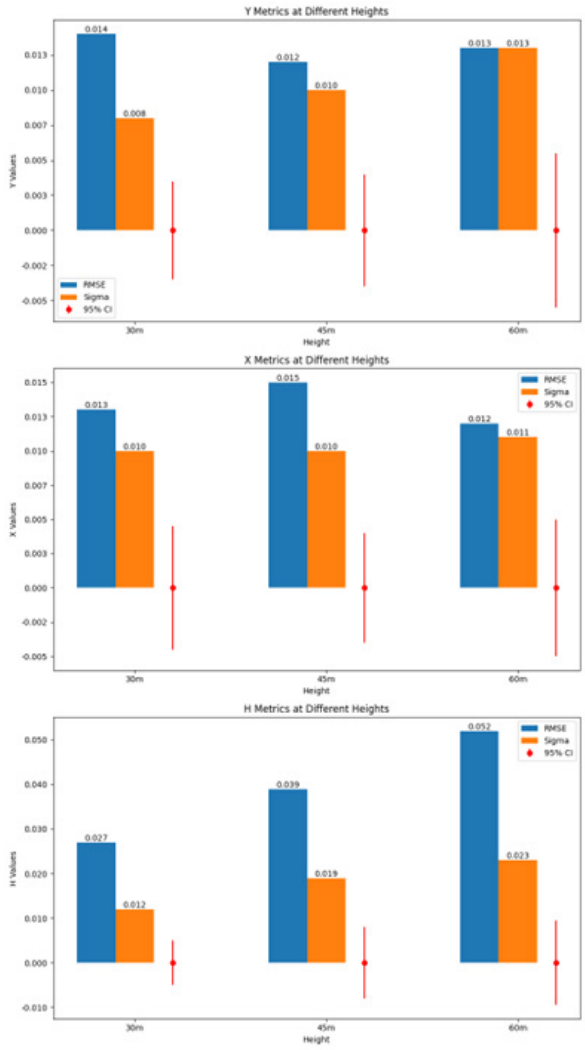

Figure 6. RMSE, σ and confidence intervals (95%) for all altitudes.

According to Figure 6, similar RMSE and σ values were calculated for the Y and X coordinate differences at 30 m and 45 m, an increase in RMSE and sigma values was observed for the H axis. This indicates that there is more deviation in the H coordinate measurements as the height increases, which is supported by the statistical test results (Table 5). Also, the 95% confidence intervals provide important information for assessing the reliability and accuracy of the measurements. Particularly at the 60 m height, the wide confidence interval and high RMSE value for the H coordinate suggest that measurements at this height require careful assessment.

DISCUSSION

In this study, the 3D coordinates of 22 CPs were calculated as the average of two different GNSS sessions and results were accepted as reference coordinates for further evaluations. Then, autonomous photogrammetric flights were conducted at 30, 45, and 60 meters in the same test field using a Mavic 3E UAV. The data obtained from those flights were processed using Pix4D software to create point clouds for each flight. The 3D coordinates of CPs were determined using the models. Those two data sets were analyzed for statistical significance. Photogrammetric models derived from different UAV altitudes enable comparison of the precision and accuracy of the data sets. Here, the RTK capabilities of the Mavic 3E UAV and the Pix4D software made it possible to create highly accurate 3D models. Calculating the differences between the GNSS data and photogrammetric models and statistically analyzing those differences provide ability to evaluate the reliability and accuracy of different methodologies.

This study aims to examine the coordinate differences between GNSS and photogrammetric data, demonstrating the accuracy and reliability of photogrammetric methods. Additionally, the results provide crucial information for evaluating UAV-based photogrammetry in large-scale mapping projects. In this context, the comparisons also contribute to identifying necessary improvements to enhance the accuracy of photogrammetric models.

Statistical Analysis

The Shapiro-Wilk test was applied to evaluate the normal distribution of all data sets. The results of this test led to the selection of appropriate statistical tests and enhanced the accuracy of the analytical process. Then, the paired t-test was used for differences with normal distribution, while the non-parametric Wilcoxon test was applied for the data outside of that kind. Those statistical tests are critical for assessing the accuracy and reliability of photogrammetric flights conducted at different altitudes. Additionally, the RMSE, confidence intervals, and σ values were used to determine the numerical variances of coordinate differences and the reliability of photogrammetric flights. RMSE values help to assess the magnitude of the errors in each axis, while confidence intervals indicate the statistical reliability and precision of the results. σ values measure the spread and degree of deviation in the data, playing a crucial role in comparing UAV flights.

Those comprehensive statistical analyses allowed for an in-depth examination of the reliability and accuracy of the data obtained from the flights. Understanding the numerical variances of coordinate differences is essential for evaluating the performance of the flights conducted at different altitudes. Also, RMSE, confidence intervals, and σ values facilitate a thorough interpretation of the results. Those analyses have established a significant basis for comparing the precision of photogrammetric methods and GNSS measurements.

Findings

The results indicate systematic and significant differences between the GNSS measurements, and the photogrammetric models conducted at 30 m and 45 m altitudes. For the 60 m flight, the errors in the Y and X axes were random, while the H differences remained significant and systematic, as observed in the other photogrammetric models. Those results are crucial in terms of the usability of photogrammetric models in projects requiring high accuracy. Regulatory standards, in particular, stipulate that differences between horizontal and

vertical coordinates should not exceed ±7 cm in large-scale map production, thus, almost all the differences are below these limits, especially for 30 m and 45 m UAV models. Those results indicate that GCP establishment in the field may not be essential while using RTK-UAVs. This step is significant to ensure both compliance with existing regulations and to obtain higher accuracy data.

Regulatory Implications

According to Türkiye's "Regulation on the Production of Large-Scale Maps and Map Information," the differences between reference and observed coordinates must not exceed ±7 cm in both horizontal and vertical values (22). The results demonstrate that photogrammetric models can achieve better accuracy than the specified limit. This suggests that UAV-based photogrammetry, using embedded RTK modules, can be utilized as an alternative to traditional GNSS-based methods for certain applications. The UAV data collection without the use of any GCPs in the field may eliminate the necessity for rapid/static GNSS observations at any ground point in the field. This may require updating the relevant articles of the regulation to reflect current conditions.

The accuracy of photogrammetric models satisfying the regulatory limits enhances the potential of UAV use in large-scale mapping projects. This can accelerate the data-gathering process and reduce costs in areas where field conditions are challenging or with limited access. For instance, UAVs can collect data more quickly and reliably than traditional methods in areas such as forests, mountainous regions, or urban areas.

Furthermore, the RTK-UAV approach can offer significant advantages in fields such as disaster management, agriculture, urban planning, and environmental monitoring. This technology's rapid data collection and analysis capabilities can provide assistance for quick responses in emergencies and expedite decision-making processes. Additionally, in agriculture, this technique may contribute to the development of precision farming applications such as plant health monitoring and yield prediction.
Updating current regulations and eliminating the GCP should cover not only the accuracy criteria for photogrammetric methods of this kind but also the standards for equipment and software used in data collection processes. That will enable more consistent and reliable data acquisition for all stakeholders.

CONCLUSION

This study highlights the potential of using RTK-embedded UAVs to achieve high-accuracy 3D positioning similar to traditional GNSS techniques without the need for any GCPs in the field. The results demonstrate that UAV-based photogrammetry can provide reliable and precise measurements, making it a viable alternative for various geospatial applications.

Furthermore, it is suggested that the current regulations in Türkiye should be updated to accommodate advancements in UAV technology. The existing regulations are primarily designed with traditional surveying methods in mind and may not fully reflect the capabilities and advantages of modern UAV systems. Updating the regulations could significantly reduce the time and effort required for large-scale map production, thereby enhancing efficiency and cost-effectiveness. This is particularly important in contexts where rapid data collection and processing are critical, such as disaster response, urban planning, and environmental monitoring.

Future research should focus on further enhancing the capabilities of UAV photogrammetry, specifically improving the accuracy of photogrammetric models in H axis. This may involve refining the algorithms used for data processing and exploring new methods for integrating UAV data with other geospatial data sets.

Additionally, optimizing UAV flight parameters and RTK capabilities is of critical importance. The impact of different flight altitudes, speeds, and patterns on data accuracy and reliability can help developing best practices for UAV operations in various environments under different conditions. In conclusion, this study reveals that RTK-based UAV photogrammetry is a reliable and effective tool for large-scale map production and other applications, meeting regulatory requirements and without GCP establishment. Updating the regulations will facilitate the wider use of this technology and make map production processes more efficient and less time-consuming.

References

1. Pu S, Vosselman G. Knowledge-based reconstruction of building models from terrestrial laser scanning data. ISPRS J Photogramm Remote Sens. 2009;64(6):575–84. doi: 10.1016/j.isprsjprs.2009.04.001.
2. Leite F, Akcamete A, Akinci B, Atasoy G, Kiziltas S. Analysis of modeling effort and impact of different levels of detail in building information models. Autom Constr. 2011;20:601–9. doi: 10.1016/j.autcon.2010.11.027.
3. Quagliarini E, Clini P, Ripanti M. Fast, low-cost and safe methodology for the assessment of the state of conservation of historical buildings from 3D laser scanning: The case study of Santa Maria in Portonovo (Italy). J Cult Herit. 2017;24:175–83. doi: 10.1016/j.culher.2016.10.006.
4. Taddia Y, González-García L, Zambello E, Pellegrinelli A. Quality assessment of photogrammetric models for façade and building reconstruction using DJI Phantom 4 RTK. Remote Sens. 2020;12(19):3144. doi: 10.3390/rs12193144.
5. Day D, Weaver W, Wilsing L. Accuracy of UAS photogrammetry: A comparative evaluation. Photogramm Eng Remote Sensing. 2016;82(12):909-14. doi: 10.14358/PERS.82.12.909.
6. Sanz-Ablanedo E, Chandler JH, Rodríguez-Pérez JR, Ordóñez C. Accuracy of unmanned aerial vehicle (UAV) and SfM photogrammetry survey as a function of the number and location of ground control points used. Remote Sens. 2018;10(10):1606. doi: 10.3390/rs10101606.
7. Elkhrachy I. Accuracy assessment of low-cost unmanned aerial vehicle (UAV) photogrammetry. Alexandria Eng J. 2021;60:5579–90. doi: 10.1016/j.aej.2021.04.011.
8. Ansari A. Use of point cloud with a low-cost UAV system for 3D mapping. In: Proceedings of the 2012 International Conference on Emerging Trends in Electrical Engineering and Energy

Management (ICETEEEM); 2012 Dec 13-15; Chennai, India. IEEE; 2012. p. 131-134. doi: 10.1109/ICETEEEM.2012.6494471.
9. Daponte P, De Vito L, Mazzilli G, Picariello F, Rapuano S. A height measurement uncertainty model for archaeological surveys by aerial photogrammetry. Measurement. 2017;98:192-8. doi: 10.1016/j.measurement.2016.11.033.
10. Sun S, Wang B. Low-altitude UAV 3D modeling technology in the application of ancient buildings protection situation assessment. Energy Procedia. 2018;153:320–4. doi: 10.1016/j.egypro.2018.10.082.
11. Vitale V. The case of the middle valley of the Sinni (Southern Basilicata). Methods of archaeological and architectural documentation: 3D photomodelling techniques and use of RPAS. Digit Appl Archaeol Cult Herit. 2018;11:e00084. doi: 10.1016/j.daach.2018.e00084.
12. Zheng X, Wang F, Li Z. A multi-UAV cooperative route planning methodology for 3D fine-resolution building model reconstruction. ISPRS J Photogramm Remote Sens. 2018;146:483–94. doi: 10.1016/j.isprsjprs.2018.11.004.
13. Mavroulis S, Andreadakis E, Spyrou NI, Antoniou V, Skourtsos E, Papadimitriou P, et al. UAV and GIS-based rapid earthquake-induced building damage assessment and methodology for EMS-98 isoseismal map drawing: The June 12, 2017 Mw 6.3 Lesvos earthquake. Int J Disaster Risk Reduct. 2019;37:101169. doi: 10.1016/j.ijdrr.2019.101169.
14. Jones CA, Church E. Photogrammetry is for everyone: Structure-from-motion software user experiences in archaeology. J Archaeol Sci Rep. 2020;30:102261. doi: 10.1016/j.jasrep.2020.102261.
15. Hill AC, Laugier EJ, Casana J. Archaeological remote sensing using multi-temporal, drone-acquired thermal and near infrared (NIR) imagery: A case study at the Enfield Shaker Village, New Hampshire. Remote Sens. 2020;12(4):690. doi: 10.3390/rs12040690.
16. Ekaso D, Nex F, Kerle N. Accuracy assessment of real-time kinematics (RTK) measurements on unmanned aerial vehicles (UAV) for direct geo-referencing. Geo-Spatial Inf Sci. 2020;23(2):165–81. doi: 10.1080/10095020.2019.1710437.
17. Eltner A, Sofia G. Structure from motion photogrammetric technique. Developments in Earth Surface Processes. Amsterdam: Elsevier; 2020. Vol. 23, p. 1–24. doi: 10.1016/B978-0-444-64177-9.00001-1.
18. Stott E, Williams RD, Hoey TB. Ground control point distribution for accurate kilometre-scale topographic mapping using an RTK-GNSS unmanned aerial vehicle and SfM photogrammetry. Drones. 2020;4(3):55. doi: 10.3390/drones4030055.
19. Benassi F, Dall'Asta E, Diotri F, Forlani G, di Cella UM, Roncella R, et al. Testing accuracy and repeatability of UAV blocks oriented with GNSS-supported aerial triangulation. Remote Sens. 2017;9(2):172. doi: 10.3390/rs9020172.
20. Varbla S, Puust R, Ellman A. Accuracy assessment of RTK-GNSS equipped UAV conducted as-built surveys for construction site modelling. Surv Rev. 2020;53(381):477–92. doi: 10.1080/00396265.2020.1830544.
21. TMMOB Harita ve Kadastro Mühendisleri Odası. Büyük Ölçekli Harita ve Harita Bilgileri Üretim Yönetmeliği [Internet]. Ankara: TMMOB Harita ve Kadastro Mühendisleri Odası; 2018. [cited 2024 Nov 25] Available from: https://www.harita.gov.tr/uploads/files/regulations/buyuk-olcekli-harita-ve-harita-bilgileri-uretim-yonetmeligi-65.pdf
22. Pix4D. Pix4D Documentation [Internet]. [cited 2024 Nov 25] Available from: https://support.pix4d.com/hc/en-us/articles/202557489
23. TUSAGA-AKTİF. Türkiye Ulusal Sabit GNSS Ağı-Aktif. [cited 2024 Nov 25] Available from: https://www.tusaga-aktif.gov.tr/
24. Harwin S, Lucieer A. Assessing the accuracy of georeferenced point clouds produced via multi-view stereopsis from unmanned aerial vehicle (UAV) imagery. Remote Sens. 2012;4(6):1573–99. doi: 10.3390/rs4061573.
25. Štroner M, Urban R, Reindl T, Seidl J, Broucek J. Evaluation of the georeferencing accuracy of a photogrammetric model using a quadrocopter with onboard GNSS RTK. Sensors. 2020;20(8):2318. doi: 10.3390/s20082318.
26. Taddia Y, Stecchi F, Pellegrinelli A. Using DJI Phantom 4 RTK drone for topographic mapping of coastal areas. ISPRS Int Arch Photogramm Remote Sens Spat Inf Sci. 2019;XLII-2/W13:625–30. doi: 10.5194/isprs-archives-XLII-2-W13-625-2019.
27. James MR, Robson S, d'Oleire-Oltmanns S, Niethammer U. Optimising UAV topographic surveys processed with structure-from-motion: Ground control quality, quantity and bundle adjustment. Geomorphology. 2017;280:51–66. doi: 10.1016/j.geomorph.2016.11.021.
28. Woodget AS, Carbonneau PE, Visser F, Maddock IP. Quantifying submerged fluvial topography using hyperspatial resolution UAS imagery and structure from motion photogrammetry. Earth Surf Process Landf. 2015;40:47–64. doi: 10.1002/esp.3613.
29. Woodget AS, Austrums R, Maddock IP, Habit E. Drones and digital photogrammetry: From classifications to continuums for monitoring river habitat and hydromorphology. WIREs Water. 2017;4:e1222. doi: 10.1002/wat2.1222.
30. Martinez-Carricondo P, Agüera-Vega F, Carvajal-Ramirez F, Mesas-Carrascosa F-J, Garcia-Ferrer A, Perez-Porras F-J. Assessment of UAV-photogrammetric mapping accuracy based on variation of ground control points. Int J Appl Earth Obs Geoinf. 2018;72:1–10. doi: 10.1016/j.jag.2018.05.015.
31. Kahveci M. Kinematik GNSS ve RTK CORS Ağları. Ankara: Nobel; 2017.
32. DJI Enterprise. DJI Mavic 3 Enterprise Specs. [cited 2024 Nov 25] Available from: https://enterprise.dji.com/mavic-3-enterprise/specs
33. Enterprise. DJI Terra. [cited 2024 Nov 25] Available from: https://enterprise.dji.com/dji-terra
34. Gehan EA. A generalized Wilcoxon test for comparing arbitrarily singly-censored samples. Biometrika. 1965;52(1-2):203–24. doi: 10.1093/biomet/52.1-2.203.
35. Shapiro SS, Wilk MB. An analysis of variance test for normality (complete samples). Biometrika. 1965;52(3-4):591–611. doi: 10.2307/2333709.
36. Hedberg EC, Ayers S. The power of a paired t-test with a covariate. Soc Sci Res. 2015;50:277–91. doi: 10.1016/j.ssresearch.2014.12.004.